IOPscience iopscience.iop.org

Home Search Collections Journals About Contact us My IOPscience

The effect of elemental substitution on the electronic properties of Ru_2Ge_3

This article has been downloaded from IOPscience. Please scroll down to see the full text article.

2002 J. Phys.: Condens. Matter 14 6543

(http://iopscience.iop.org/0953-8984/14/25/321)

View the table of contents for this issue, or go to the journal homepage for more

Download details:
IP Address: 171.66.16.96
The article was downloaded on 18/05/2010 at 12:10

Please note that terms and conditions apply.

INSTITUTE OF PHYSICS PUBLISHING JOURNAL OF PHYSICS: CONDENSED MATTER

J. Phys.: Condens. Matter **14** (2002) 6543–6552 PII: S0953-8984(02)33645-2

The effect of elemental substitution on the electronic properties of Ru_2Ge_3

M A Hayward[1] **and R J Cava**

Department of Chemistry, Princeton Materials Institute, Princeton University, Princeton, NJ 08544, USA

E-mail: mhayward@princeton.edu

Received 11 February 2002, in final form 8 May 2002
Published 14 June 2002
Online at stacks.iop.org/JPhysCM/14/6543

Abstract
The effect of chemical substitution on the electrical resistivity and Seebeck coefficients of Ru_2Ge_3 is reported, with a particular emphasis on enhancing the properties relevant to thermoelectric behaviour. The properties of Ru_2Ge_3 itself are shown to be strongly dependent on quenching temperature. The effects of metal doping for Ru and metalloid substitution (Sn and Si) for Ge are reported. It is shown that doping of both ruthenium and germanium sites is required to reduce the high resistivity of Ru_2Ge_3 (~280 mΩ cm at 300 K) to a value of 1.5 mΩ cm, for $Ru_{1.85}Mn_{0.15}Ge_{2.4}Sn_{0.6}$ while maintaining high Seebeck coefficients. This latter composition has the highest thermoelectric figure of merit observed in this system: $ZT_{300\ K} = 1 \times 10^{-2}$. Unfortunately this value is too small to be competitive with existing materials.

1. Introduction

The difficulty in preparing efficient thermoelectric materials is characterized by the need to minimize the thermal conductivity of candidate materials, while maximizing their electronic conductivity. The traditional strategy to optimize these conflicting parameters involves selecting semiconducting compounds containing heavy elements and then reducing their thermal conductivity by introducing crystallographic disorder. The introduction of the concept of a phonon-glass–electron-crystal (PGEC) material, most notably by Slack [1], provides an alternative strategy. The PGEC concept describes a material which has an open semiconducting or semimetallic framework (electron crystal) containing loosely bound guest atoms (phonon glass). These guest atoms rattle within the framework producing low frequency anharmonic modes, which strongly scatter the heat carrying acoustic modes of the material, thus reducing the thermal conductivity to glass-like values without serious detriment to the electronic conductivity. Thus one could produce efficient thermoelectric materials by optimizing the

[1] Author to whom any correspondence should be addressed.

electronic properties of such a PGEC material by utilizing the already low thermal conductivity of such a phase.

A material worthy of such attention is the Nowotny chimney–ladder phase Ru_2Ge_3. The combination of a two-component structure, low thermal conductivity and semiconducting transport behaviour [2] make it a good candidate for the optimization of thermoelectric properties by elemental substitution. Here we report a study of the electronic properties of Ru_2Ge_3 that are the result of such substitutions. The resistivity of these materials is particularly sensitive to substitution and the exact preparative conditions employed.

2. Experimental details

In order to investigate the effect of elemental substitution on the electronic properties of Ru_2Ge_3, relevant to thermoelectricity, a large number of samples of the composition $Ru_{2-x}A_xGe_{3-y}B_y$ were prepared. Samples of approximate mass 0.5 g were prepared by arc melting appropriate amounts of the constituent elements, three times under argon. The melted buttons were then individually wrapped in Ta foil, sealed in evacuated quartz ampoules and annealed for 7 days at 950 °C. The ampoules were then quenched to room temperature in water. A number of samples were annealed and subsequently quenched from lower temperatures, as described in the text, in order to determine the effect of annealing temperature on sample properties. Samples were weighed prior to and after annealing to confirm that no material was lost during sample preparation (maximum observed mass loss: 0.3%).

The phase purity of the annealed samples was assessed by x-ray powder diffraction (Rigaku Miniflex, Cu Kα radiation). The annealed buttons were cut into bars (approximate dimensions: 1 mm $\times$ 1 mm $\times$ 4 mm) which were employed in resistivity and Seebeck coefficient measurements. Resistivity measurements were performed using a standard four-point ac method utilizing a Quantum Design PPMS instrument. The Seebeck coefficients of samples were measured using commercially available apparatus (MMR technologies). ZT measurements were made using Harman's method [3].

3. Results

3.1. Quenching temperature

Ru_2Ge_3 is reported to undergo a continuous diffusionless phase transition below $\approx$500 °C [4]. This transition involves displacement of the germanium atoms within the quasi-static ruthenium lattice, resulting in a change of crystallographic symmetry from a high temperature tetragonal form ($P\bar{4}2c$) to a low temperature orthorhombic form (*Pbcn*). Stoichiometric samples of Ru_2Ge_3 which were annealed at 950 °C and then for one week at lower temperatures ($T = 700$, 575 and 450 °C) before quenching in water, produced single-phase samples. X-ray powder diffraction data collected from all samples could only be indexed using the low temperature orthorhombic cell reported for Ru_2Ge_3 ($a = 11.436$ Å, $b = 9.238$ Å, $c = 5.716$ Å [5]). There is no crystallographic evidence in any of the samples for the existence of a tetragonal form of Ru_2Ge_3. This suggests that it is not possible to quench the tetragonal form.

Figure 1(a) shows the effect of quenching temperature on the resistivity and Seebeck coefficients (figure 1(b)) of Ru_2Ge_3. Both data sets show a clear discontinuity between samples quenched at 575 and 450 °C consistent with the reported crystallographic phase transition. The resistivity of Ru_2Ge_3 has little dependence on the quenching temperature in samples quenched from $T \geqslant 700$ °C, prior to a sharp increase in resistivity as the phase transition is approached. Figure 2(a) shows that the Seebeck coefficients of the samples decrease steadily with decreasing

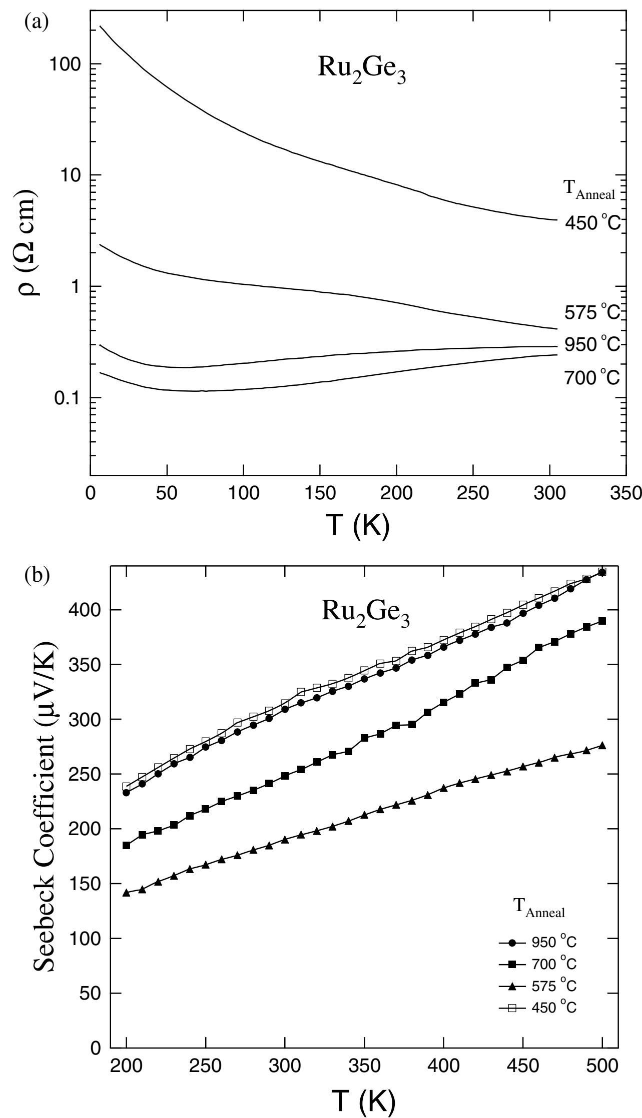

Figure 1. Effect of quenching temperature on (a) resistivity and (b) Seebeck coefficient of Ru_2Ge_3.

quenching temperature prior to a sharp increase between samples quenched at 575 and 450 °C. Combining both data sets allows us to calculate the thermoelectric 'power factor', S^2/ρ, often used as a measure of the electronic factors that contribute to optimal thermoelectric performance [6]. Figure 2(b) shows that samples quenched from high temperature have significantly higher power factors than those annealed at low temperatures. Therefore all subsequent samples were quenched from 950 °C.

3.2. Ru-site doping

Figure 1 shows that the best room temperature resistivities attained for undoped Ru_2Ge_3 are ≈200 mΩ cm. This is approximately two orders of magnitude larger than those of

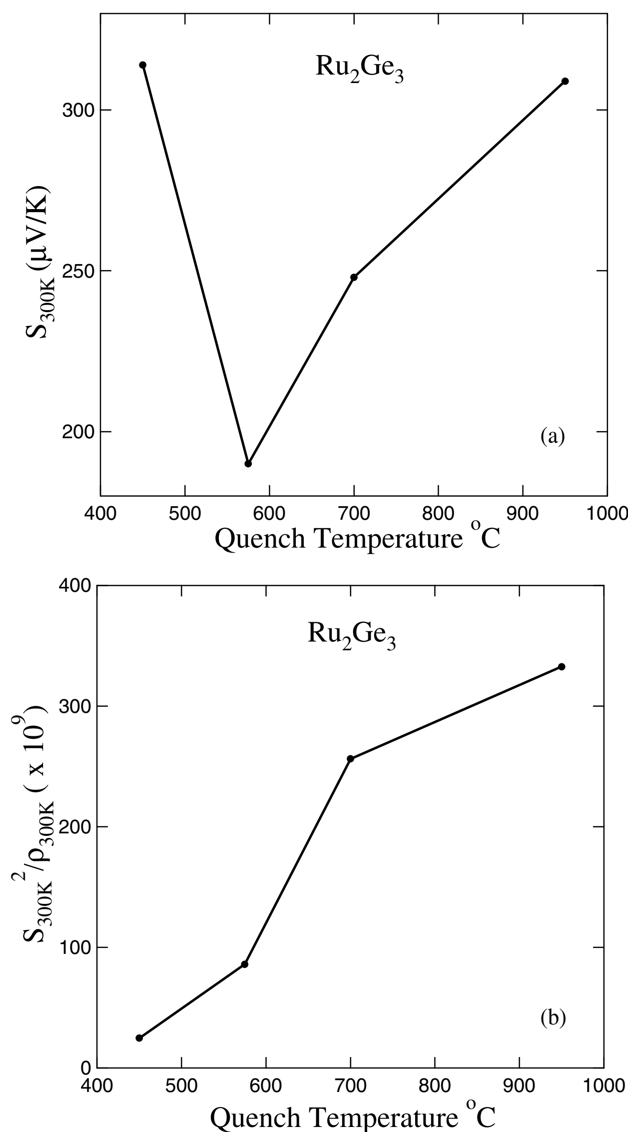

Figure 2. Plot of (a) Seebeck coefficient at 300 K and (b) power factor at 300 K as a function of quenching temperature for Ru_2Ge_3.

good thermoelectric materials. In order to lower this value, elemental substitution for ruthenium was performed. Figure 3 shows the temperature dependence of the resistivity of samples of composition $Ru_{1.95}M_{0.05}Ge_3$ (M = Ni, Pt, Mn, Co, Fe). The data in figure 3 show that the resistivity of the doped samples is slightly reduced with respect to undoped Ru_2Ge_3; however, all samples still have resistivities too large to make effective thermoelectric materials ($\rho_{300\ \mathrm{K}} > 100$ mΩ cm). In addition the data show that with the exception of the cobalt-doped sample, the resistivities of all the doped materials display the same weak temperature dependence exhibited by Ru_2Ge_3. This behaviour is characteristic of materials in which impurity bands dominate the electronic transport, as is the case with undoped

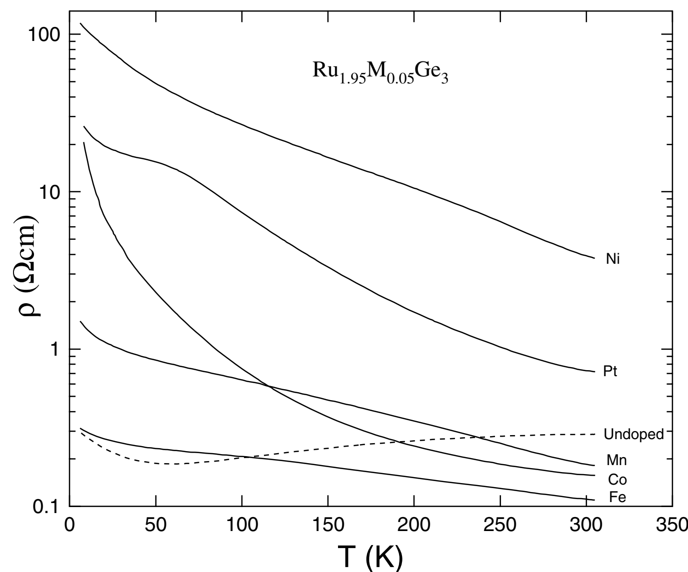

Figure 3. Plot of the temperature dependence of the resistivity of doped Ru_2Ge_3 samples of formula $Ru_{1.95}M_{0.05}Ge_3$.

Ru_2Ge_3. The resistivity data collected from the cobalt-doped sample do have the temperature dependence characteristic of activated behaviour. Extracting the apparent bandgap from the slope of a plot of $-\ln\sigma$ against $1/2k_BT$ yields a value of 0.04 eV. This is much smaller than the high temperature value reported for Ru_2Ge_3 (0.34 eV [2]) suggesting that the observed gap involves a band of impurity states, which lies between the valence and conduction bands. The involvement of impurity states in the transport behaviour of all samples suggests that it will not be possible to significantly reduce the resistivity of Ru_2Ge_3 by simple substitution for ruthenium, as this does not overcome the inherent problem of the observed low carrier mobility of these impurity states.

3.3. Ge-site doping

An alternative method of reducing the resistivity of Ru_2Ge_3 is by elemental substitution on the germanium site. Susz *et al* [2] report that Ru_2Si_3 and to a limited extent Ru_2Sn_3 are soluble in Ru_2Ge_3. Investigation of the electronic properties of these materials reveals a decease in the electronic bandgap from Ru_2Si_3 (0.7 eV) to Ru_2Ge_3 (0.34 eV) to Ru_2Sn_3 (metallic) [2]. Such a trend should in principle allow the tuning of the electronic bandgap to optimize the thermoelectric properties of this system. X-ray powder diffraction data collected for samples of stoichiometry $Ru_2Ge_{3-x}Si_x$ ($x = 0, 1, 2, 3$) showed that all samples reacted to form single-phase materials with structures and lattice parameters consistent with a solid solution between the reported structures of Ru_2Ge_3 and Ru_2Si_3. Conversely there is a solubility limit in the substitution of germanium with tin in Ru_2Ge_3. For values of $x > 0.6$ the samples of initial stoichiometry $Ru_2Ge_{3-x}Sn_x$ displayed diffraction peaks due the phase Ru_3Sn_7. This impurity phase could not be removed, even with annealing times in excess of 7 days. Therefore only the physical properties of $Ru_2Ge_{3-x}Sn_x$ samples with $x \leqslant 0.6$ were measured.

Figure 4 shows the resistivity and Seebeck coefficients of samples of composition $Ru_2Ge_{3-x}M_x$ (M = Si, Sn) plotted against temperature. The observed trend that the resistivity

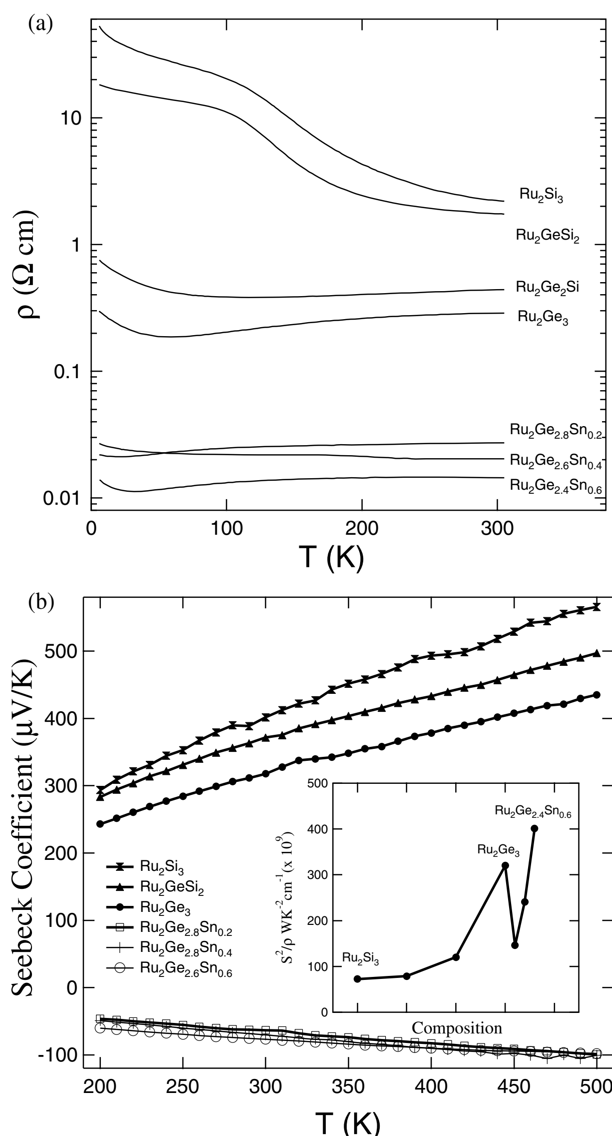

Figure 4. Plot of the temperature dependence of (a) the resistivity and (b) the Seebeck coefficients of doped Ru_2Ge_3 samples of formula $Ru_2Ge_{3-x}M_x$ (M = Si, Sn). The inset to (b) shows the power factor of samples at 300 K as a function of composition.

reduces from $Ru_2Si_3 > Ru_2Ge_3 > Ru_2Sn_3$ is in agreement with the data previously reported and can be rationalized by observing that the electronic bandgaps of the materials follow the same trend [2]. The temperature dependence of the resistivity evolves from that of Ru_2Si_3 and Ru_2GeSi_2, which display thermally activated behaviour in the temperature range $100 < T$ (K) < 300, to the tin-doped samples that, in common with Ru_2Ge_3, have only a weak variation with temperature. The apparent bandgaps extracted for Ru_2Si_3 and Ru_2GeSi_2, 0.074 and 0.065 eV respectively, show that in common with all the samples in this series impurity states have a dominant effect on the transport behaviour in the temperature range studied.

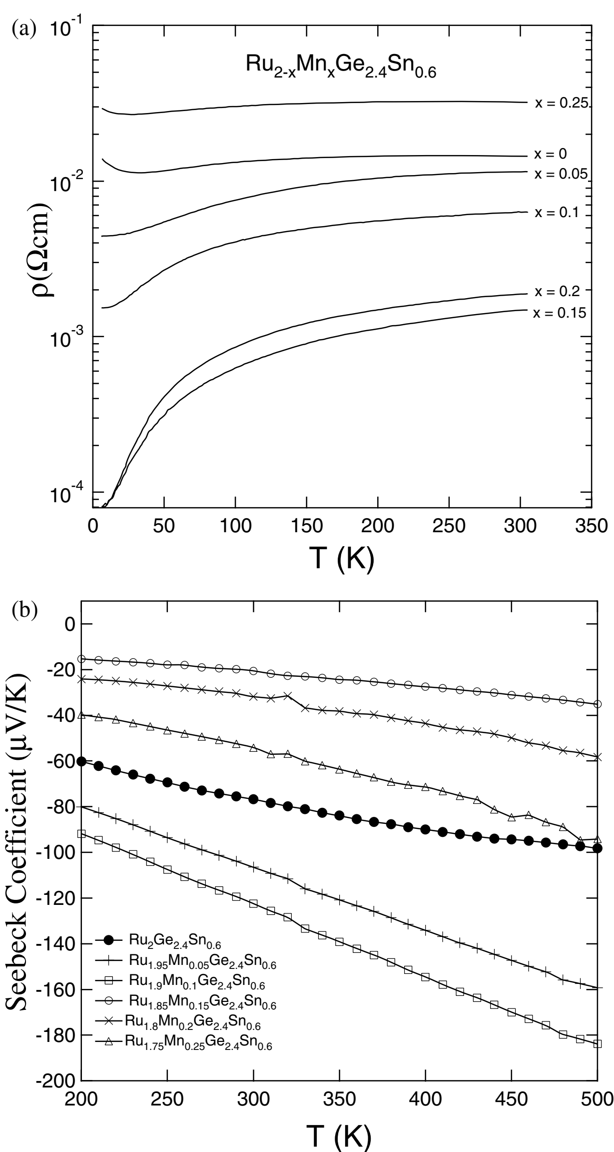

Figure 5. Plot of the temperature dependence of (a) the resistivity and (b) the Seebeck coefficients of samples of formula $Ru_{2-x}Mn_xGe_{2.4}Sn_{0.6}$.

Figure 4(b) shows the Seebeck coefficients for the $Ru_2Ge_{3-x}M_x$ (M = Si, Sn) series. It can be seen that Seebeck coefficients of all the samples increase smoothly and continuously with temperature in the range measured. In the series $Ru_2Ge_{3-x}Si_x$ the Seebeck coefficients of samples increase with increasing x from $S_{300\ K} = 317\ \mu V\ K^{-1}$ for Ru_2Ge_3 to $S_{300\ K} = 401\ \mu V\ K^{-1}$ for Ru_2Si_3. Such an increase is consistent with the reported increase in the electronic bandgap which would lead to a reduction in the number of charge carriers and the observed increase in both the Seebeck coefficient and electronic resistivity with increased silicon content.

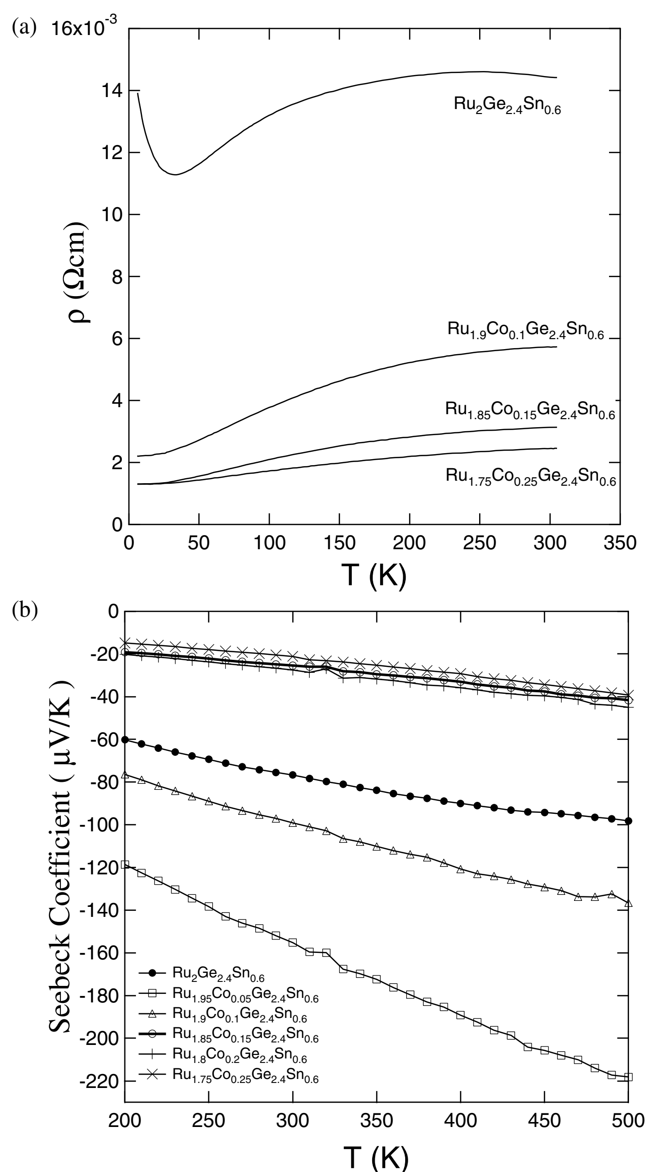

Figure 6. Plot of the temperature dependence of (a) the resistivity and (b) the Seebeck coefficients of samples of formula $Ru_{2-x}Co_xGe_{2.4}Sn_{0.6}$.

The substitution of small amounts of tin for germanium leads to a change of sign of the Seebeck coefficient. This indicates a change in the dominant charge carriers from holes to electrons. Associated with this change in carrier type is a reduction in the absolute magnitude of the Seebeck coefficient. The net effect of Ge site doping can be seen in the inset to figure 4(b) which plots the power factor, S^2/ρ, against composition. This clearly shows that after a local maximum at undoped Ru_2Ge_3, the power factor increases with Sn content. Despite this trend $Ru_2Ge_{2.4}Sn_{0.6}$ (the maximum Sn content soluble in Ru_2Ge_3) is not an effective thermoelectric material ($ZT_{300\ K} \sim 2.3 \times 10^{-3}$ estimated by Harman's method [3]) as the electronic resistivity is still restrictively large.

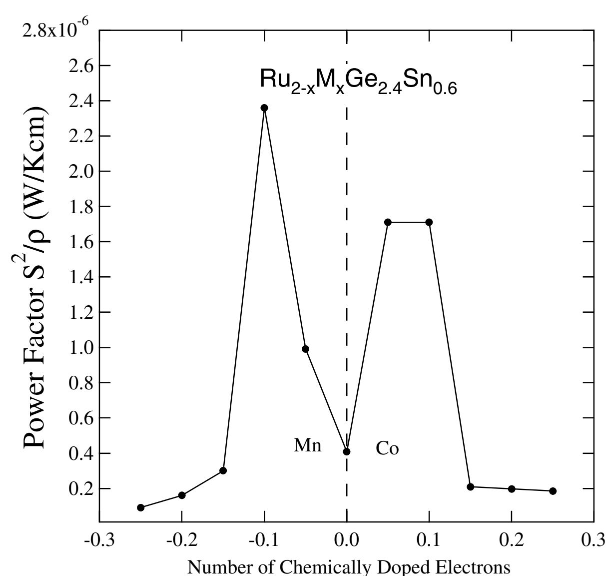

Figure 7. Plot of the power factor at 300 K as a function of composition in samples of formula $Ru_{2-x}M_xGe_{2.4}Sn_{0.6}$ (M = Mn, Co).

3.4. Double-site doping

In order to complete the characterization of the resistivity and Seebeck coefficients in this system, samples doped on both the Ru and Ge sites were prepared based on the maximal power factor of $Ru_2Ge_{2.4}Sn_{0.6}$. Figures 5 and 6 show the temperature dependence of the resistivity and Seebeck coefficients of samples of composition $Ru_{2-x}M_xGe_{2.4}Sn_{0.6}$ (M = Mn, Co, $0 < x < 0.25$). It can be seen that in both the Mn- and Co-doped samples low levels of substitution for ruthenium lead to a rapid drop in resistivity to values of the order of 1 mΩ cm at 300 K. Substitution with cobalt (figure 5(a)) lowers the resistivity in a continuous manner with increasing cobalt concentration leading to a steady reduction in sample resistivity. Conversely doping samples with Mn (figure 6(a)) initially leads to a drop in resistivity, with a local minimum around $x = 0.15$, before rising sharply at higher Mn concentrations. The Seebeck coefficients of the Mn- and Co-doped samples (figures 5(b) and 6(b)) both show the same type of behaviour. Small dopant concentrations lead to a rise in the absolute magnitude of the Seebeck coefficients of both sets of samples, reaching local maxima at $x = 0.05$ and 0.1 for the Co- and Mn-doped samples respectively. At higher doping levels the Seebeck coefficients of both sets of samples drop to around 20 μV K^{-1} at 300 K. It should be noted that despite Mn being a formal hole dopant and Co being a formal electron dopant, both materials give large negative Seebeck coefficients indicating negative charge carriers dominate the transport in both sets of materials.

Figure 7 plots the power factors of the $Ru_{2-x}M_xGe_{2.4}Sn_{0.6}$ samples against the number of holes or electrons chemically doped into the sample per formula unit (Mn can be considered a formal hole dopant, Co a formal electron dopant). It can clearly be seen that the largest power factors are achieved when small numbers of holes or electrons are doped into $Ru_2Ge_{2.4}Sn_{0.6}$, with the local maxima located at $Mn_{0.1}$ and $Co_{0.05}$ respectively.

Utilizing Harman's method to estimate the value of ZT at room temperature, values of 1×10^{-2} and 8.51×10^{-3} are evaluated for the $Mn_{0.1}$ and $Co_{0.05}$ materials respectively.

These values mirror the power factors shown in figure 7. Harman's method measures the overall figure of merit, $ZT = T\rho S^2/\kappa$, and so the scaling of ZT with power factor suggests that the materials have similar thermal conductivities which we deduce to be $\kappa_{300} \approx 0.065$ W K^{-1} cm^{-1}.

4. Conclusion

We have reported the effects of elemental substitution on the electronic properties of Ru_2Ge_3, relevant to its potential as a thermoelectric material. It has been possible, by substituting on both the Ru and Ge sites, to reduce the electrical resistivity of Ru_2Ge_3 by two orders of magnitude, from 280 mΩ cm at 300 K in undoped Ru_2Ge_3 to 1.5 mΩ cm at 300 K in $Ru_{1.85}Mn_{0.15}Ge_{2.4}Sn_{0.6}$. However, despite this dramatic reduction in resistivity the thermoelectric figure of merit, ZT, has only been increased to 1×10^{-2} at 300 K (from 3.2×10^{-3}) making this material non-competitive as a thermoelectric at room temperature, in spite of an initially promising combination of properties. Future studies of the magnetic properties of these materials may be of interest, as the metal dopants appear to have largely created distinct primary localized states in the semiconductor host.

Acknowledgment

This work was supported by the Office of Naval Research, grant no N00014-99-1-0625.

References

[1] Slack G A 1997 *Thermoelectric Materials—New Directions and Approaches* vol478, ed TM Tritt, G Mahan, HB LyonJr and MG Kanztzidis (Pittsburgh, PA: Materials Research Society) p 47
[2] Susz C P, Muller J, Yvon K and Parthe E 1980 *J. Less-Common Met.* **71** 1–8
[3] Harman T C, Cahn J H and Logan M J 1959 *J. Appl. Phys.* **30** 1351
[4] Poutcharovsky D J, Yvon K and Parthe E 1975 *J. Less-Common Met.* **40** 139
[5] Poutcharovsky D J and Parthe E 1974 *Acta Crystallogr.* B **30** 2692
[6] Mahan G D 1997 *Solid State Phys.* **51** 81